Novel phases in ferroelectric BaTiO3 thin films

Everhardt, Arnoud

Chapter 5:

Ferroelastic domain formation by periodicity halving and periodic defects

Chapter to be submitted as peer- review article by A.S. Everhardt[1], S.-L. Zhou[1], N. Domingo[2], G. Catalan[2,3] and B. Noheda[1]

[1] Zernike Institute for Advanced Materials, University of Groningen, The Netherlands
[2] Catalan Institute of Nanoscience and Nanotechnology (ICN2), CSIC, Barcelona Institute of Science and Technology Campus, Universitat Autonoma de Barcelona, Bellaterra, 08193 Barcelona, Spain
[3] ICREA, 08193 Barcelona, Spain

Abstract

The formation of domains is the primary means to relax epitaxial strain in ferroelastic thin films. The thermodynamic laws that describe the average domain size as a function of strain (lattice mismatch and film thickness) are well established. Less understood so far is the dynamics of domain formation. In this chapter we investigate the transition between two ferroelectric phases (with a/c and a/b domain structures) as a function of temperature in thin films of $BaTiO_3$ grown on $NdScO_3$ substrates. The experiments reveal that the slow formation (annihilation) of 90 ° in-plane ferroelastic domains (a/b domains) in $BaTiO_3$ proceeds by sequential halving of the periodicity. The scaling laws of domain width versus thickness upon heating in the two domain structures points towards a model by which the domain walls of the a/b domains act as nucleation points for the a/c domains, showing the large effect of trapping by extended defects in the final domain structure. This domain periodicity halving can also explain observations in other films, where domain sizes are found to be related by a factor 2^n.

5.1 Domain width scaling

Ferroelastic materials are an interesting class of materials that display non-linear strain as a response to external stress.[1] Control of ferroelastic thin films can be achieved by utilizing epitaxial strain. The strain can be relaxed within the film by the formation of ferroelastic domains (e.g. 90 ° domains for tetragonal or orthorhombic systems).[2,3] Depending on the sign of the strain (compressive or tensile) imposed on the film by the substrate, either a/c domains (alternating in-plane and out-of-plane) or a/b (fully in-plane) domains are preferred.[4] Ferroelastic domains are expected to alternate with a certain periodicity in the absence of dislocations or other defects.

The thermodynamically most stable ferroelastic domain size as a function of film thickness was first described by Roytburd's law[2], which is based on the competition between the elastic energy in the domains and that needed for domain wall formation. It follows a square root law $w = \beta \sqrt{d}$, where w is domain size, β a prefactor and d the film thickness of an epitaxial[5] or freestanding[6] film. This square root law is more universal and also holds for ferromagnetic and ferroelectric systems with 180 ° domains[5,7] for which only the β prefactor changes significantly as it is primarily a function of domain wall thickness[8,9]: the significantly wider domain walls in ferromagnetic systems give rise to a larger β (~35 $nm^{1/2}$) than the β found for ferroelectric/ferroelastic systems (~6 $nm^{1/2}$), which have narrow domain walls.[10] Differences in β prefactors within a single type of material can also be found when the sample morphologies give different domain wall widths.[11] Deviations from the square root law are found in the very thin film limit (for domain sizes larger than the film thicknesses)[3,4], in which case the exponent n in $w = \beta d^n$ takes a value of 1[4,12]; and when there are large kinetic effects in the formation of the domains or the domain walls are irregular, for which $\frac{1}{2} < n < 1$[13,14].

The Roytburd law describes the optimal *average* domain size in thermodynamic equilibrium. The domain size measured experimentally by techniques such as X-Ray Diffraction (XRD) is also an average that, indeed, it often agrees with that determined by the above-mentioned laws[15,16]. However, locally, a large spread in domain sizes has been found by local imaging techniques such as Piezoelectric Force Microscopy (PFM) or Transmission Electron Microscopy (TEM) (some examples can be found in Refs.[14,17,18]). These differences between average and local domain size are intriguing and could help to understand the process of domain formation, which has not been well investigated because the timescale for the experimental techniques to locally measure domains is much longer than the timescale in which the domains typically form. So far only one careful study has been performed on freestanding $BaTiO_3$ films which have been measured in a 2 °C temperature range at the ferroelectric-to-paraelectric phase transition. This study has reported the kinetics of domain formation, revealing a/c domain annihilation.[19]

5.2 Domain periodicity halving

In this chapter the formation of ferroelastic/ferroelectric domains is followed by temperature-dependent PFM. The $BaTiO_3$ films used for this study have a transition at 50 °C from a ferroelectric/ferroelastic high temperature a/c domain structure to a ferroelectric/ferroelastic low temperature monoclinic ac_+^*/bc_-^* domain structure[20] (see **Chapter 4**). Since the monoclinic distortion and out of plane polarization components are rather small in this phase, for simplicity we abbreviate it to the simpler orthorhombic notation for in-plane domains: a/b.

The formation of a/b domains is slow (the full relaxation from a/c to a/b domains can take up to several days) and the transition takes place in a large temperature range, which makes it an ideal system to study with the PFM technique. The periodicity of the a/b domains at room temperature is 110 ± 10 nm (width of 60 ± 10 nm for the a-domains and of 50 ± 10 nm for the b-domains) prior to the experiments. The films are then heated to 200 °C (into the paraelectric phase) and measured during the cooldown process through the a/c and a/b phases, as shown in **Figure 5.1.** Already at 70 °C (so above the nominal a/c-to-a/b transition temperature), one b-domain has been observed

inside the a/c matrix; at 60 °C several b-domains have been found. The distances between those b-domains, 450 and 530 ± 20 nm, are much larger than the distances between b-domains found in the a/b phase at room temperature. Cooling down to 40 °C shows some dark lines appearing halfway the distance between the existing b-domains. Further cooling down to 30 °C reveals that those dark lines develop into new b-domains, reducing the distance between b-domains (to 250 ± 20 nm), which is (approximately) half of its value at 50 °C.

Further cooling down would result in another set of b-domains being formed halfway the existing ones to obtain room temperature domain sizes of 110 nm, as those before the measurement (110 nm). One can then say that the equilibrium periodicity is achieved by subsequent halving of the periodicity[21] when a new set of domains forms. Only once most of the sample has obtained the same periodicity, new domains can start forming in between the b-domains and halving of the periodicity takes place again.

In addition, it is well known that new domain walls nucleate preferentially at interfaces or other defects, such as the film surfaces or other domain walls[7], which plays an important role in the local domain size distribution. Bifurcations where two a/c domains merge into one are signalled by the arrows in **Figure 5.1d** and the circles in **Figure 5.1d-f**. All these bifurcations have a b-domain going through them, showing that they are preferred nucleation points t for new b-domains. Due to the random distribution of these defects, different domain sizes are present and even a kink (a less straight domain wall) is found for the new b-domain formed inside the red circle, due to the merger of two b-domains with different nucleation points. The b-domains can also nucleate in the existing a/c domain walls. The presence of 90 ° rotated b-domains (superdomains) helps as a nucleation point for other b-domains as seen in this data. Afterwards those superdomains can be easily rotated back to give long domains (see **Section 5.6**).[22]

A similar phase transition mechanism is observed when heating the structure from the a/b to the a/c phase, as observed in **Figure 5.2**. At 40 °C the full a/b domain structure is still intact and at 45 °C it can be seen that some b-domains have been annihilated. On further heating more and more b-domains are annihilated in line with the periodicity halving/doubling rule observed previously. Interestingly it can be seen that at 60 °C the b-domains are broken up halfway in the measurement area, rather than keeping their original long domain walls. One possibility is that the domains at the upper and lower parts of the measurement area are pinned to different defects. This indicates that the driving force for periodicity doubling is large enough to break up a domain wall.

Both these transitions show the full a/c domain pattern even when there are still many b domains present, which means that those structures are able to coexist[20]. The stress released along the a-direction should be similar for both phases (a/b and a/c) and, thus, little change is expected during the phase transition. So these transitions can be well described by considering the stress released in the b-direction (the smaller one of the anisotropic substrate lattice parameters[23]). The first b-domains formed release some stress, lowering the driving force for the formation of more b-domains. Only by lowering the temperature it is energetically favorable to form an additional set of b-domains.

New domains are preferentially being formed halfway between the existing domain walls to minimize the elastic forces on the newly created domains. It is interesting to note that the system is able to 'repair' small discrepancies in domain sizes *after* the domains have been formed. While it is impossible for all domains to change their size simultaneously once they have formed, as that would lead to massive movements of domain walls, local movements of particular domain walls are possibly driven by the stress gradients towards the middle position between existing domain walls. **Figure 5.3a** shows b-domains with different distances between the b-domains. The elastic forces in this situation lead to movement of the b-domains with respect to each other to create equal distances between the b-domains (**Figure 5.3b**).

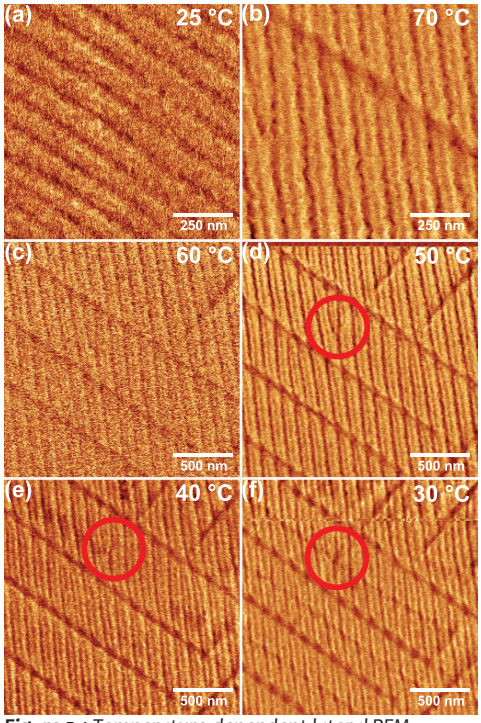

Figure 5.1 *Temperature-dependent lateral PFM (Dual AC Resonance Tracking mode) of a $BaTiO_3$ (in this case 170 nm thick) film on a $NdScO_3$ substrate.* ***a)*** *a/b domains at room temperature before the measurement. Afterwards the sample was heated to the paraelectric phase at 200 °C for 5 minutes and then cooled down in steps. Measurements were performed at 70 °C* ***(b)****, 60 °C* ***(c)****, 50 °C* ***(d)****, 40 °C* ***(e)*** *and 30 °C* ***(f)****. The red circle is signaling a bifurcation in the a/c domain structure where the new b-domain nucleates in (e), while the black arrows are signaling bifurcations where the b-domains have already formed before the measurement in (c).*

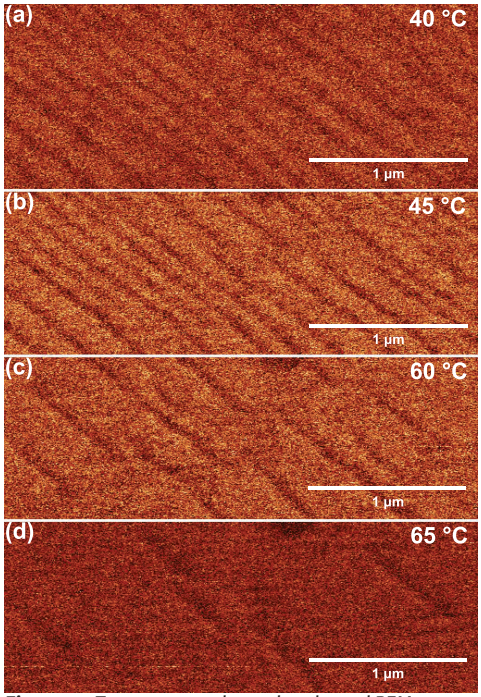

Figure 5.2 *Temperature-dependent lateral PFM (normal PFM mode) images of a $BaTiO_3$ (in this case 80 nm thick) film on a $NdScO_3$ substrate. The transition from a/b towards a/c domains is followed on heating at 40 °C* ***(a)****, 45 °C* ***(b)****, 60 °C* ***(c)*** *and 65 °C* ***(d)****. The triangular defect at the top of the image has been used to align all the images to compensate for thermal drift during the measurement.*

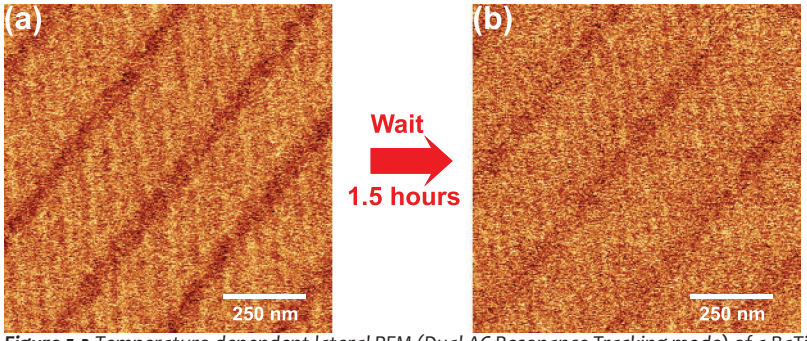

Figure 5.3 *Temperature-dependent lateral PFM (Dual AC Resonance Tracking mode) of a BaTiO3 (in this case 170 nm thick) film on a NdScO3 substrate.* ***a)*** *Five different b-domains (the dark diagonal lines) with different distances between those b-domains.* ***b)*** *After waiting for 1.5 hours, it is possible for those b-domains to move with respect to each other achieve equal distance between the b-domains.*

5.3 Thermal history-dependent scaling law

The expected quadratic Roytburd's law domain size scaling is found in **Figure 5.4a,b** for both the a/b and a/c domains with a β prefactor of about 10 $nm^{1/2}$. This is slightly larger than typical values for ferroelectric/ferroelastic systems, which probably means that the domain walls are slightly thicker than in typical ferroelectrics. However, when the a/c domains are obtained upon heating from the a/b phase, β is reduced to about 7 $nm^{1/2}$ (**Figure 5.4c**). In order to distinguish this one from the a/c domain structure found upon cooling, we call it a/c'. The a/b domain size does not depend on thermal history, which suggests that β = 10 $nm^{1/2}$ gives rise to the thermodynamic equilibrium value for both types of domains and that β = 7 $nm^{1/2}$ represents a kinetically trapped scaling law.

A model is proposed to explain the different domain sizes for the a/c and a/c' domains in **Figure 5.4d.** The domain walls for the new a/c' domains (green-dashed lines) preferably nucleate at the existing a/b domain walls (black-solid lines). Since these domain walls are rotated by 45 ° with respect to each other (with respect to an axis orthogonal to the film surface), the domain width relationship between these two domain structures is governed by a √2 factor. This would explain the two observed values for the β prefactors: β (a/b) = 10 $nm^{1/2}$ ≈ 7√2 $nm^{1/2}$ = β (a/c') √2.

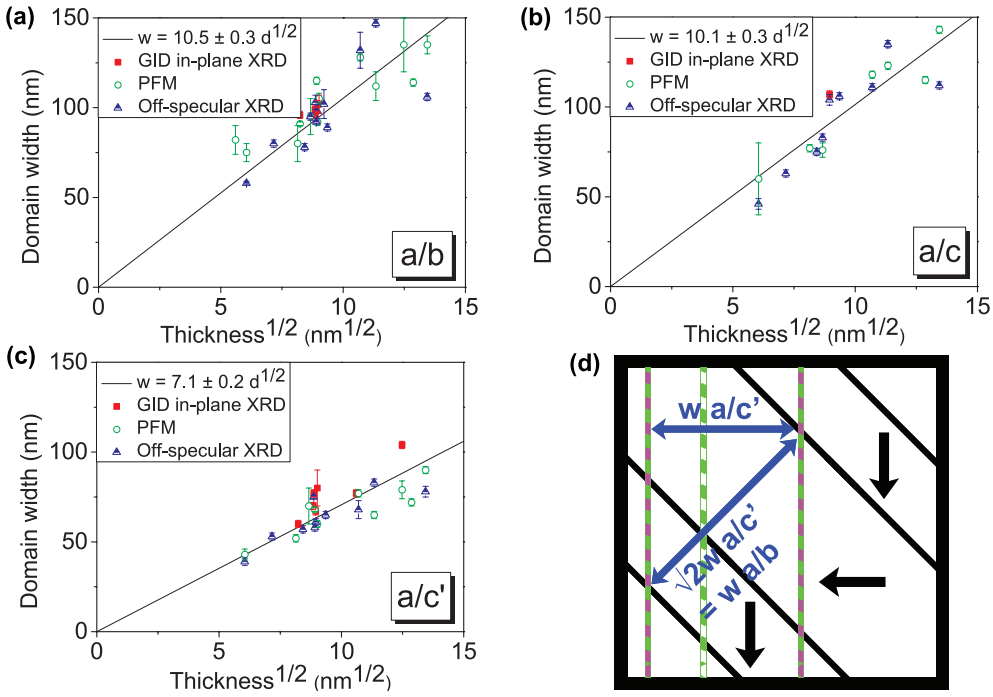

Figure 5.4 *Domain size scaling for different film thicknesses, determined by either in-plane Grazing Incidence XRD (red filled squares), off-specular (204) XRD peaks (blue half-filled triangles) or local PFM (green open circles) (methods described in Ref.[20]). The domain size is fitted to a Roytburd square root law which is given in the legend for the a/b phase* ***(a)****, for the a/c phase obtained by cooling down from the paraelectric phase* ***(b)*** *and for the a/c' phase obtained by heating from the a/b phase* ***(c)****.* ***d)*** *Drawing of the a/b matrix (black diagonal lines) with the newly formed, upon heating, a/c domain walls (green/purple dashed and green/white dashed lines are the two types of domain walls).*

5.4 Discussion

We, therefore, find that the kinetic processes have a large influence on the local domain sizes. First of all one has to consider that the first domains form at large distances from each other, where the spread of domain sizes is relatively small. However, the subsequent halving of the periodicity increases the spread of domain sizes for the final, much smaller, domains. Next to that, randomly distributed point defects can change the position where new domains nucleate. In this case, it has been shown that small movements of domain walls with respect to each other are possible to obtain their energetically more stable domain sizes. However, this is not possible when domains are pinned, by extended periodic defects, such as domain walls. This is the case with the a/c' domains described here. They are trapped because it is not possible for those domains to move all domain walls simultaneously.

The domain periodicity halving observed here for a transition between two ferroelastic domain patterns in $BaTiO_3$ can be extended to other systems. For example all the c-domains in the $PbTiO_3$ films by Nesterov et al.[14] show domain sizes of either 75, 150 or 300 nm in **Figure 5.5** and similar domain size scaling by Ganpule et al.[17] can be found in **Figure 5.6**. These discrete domain sizes are related to each other by a 2^n factor. This is most likely caused by the domain periodicity halving process, where new a-domains are preferentially form halfway between existing a-domains, thus yielding c-domain sizes that are half of those formed at the previous stage. While the domain periodicity in the $BaTiO_3$ thin films discussed in this letter can half until all domains have the same size, those other examples just mentioned in $PbZr_xTi_{1-x}O_3$ contain trapping defects that hinder subsequent periodicity halving, thus displaying a coexistence of different sizes at room temperature.

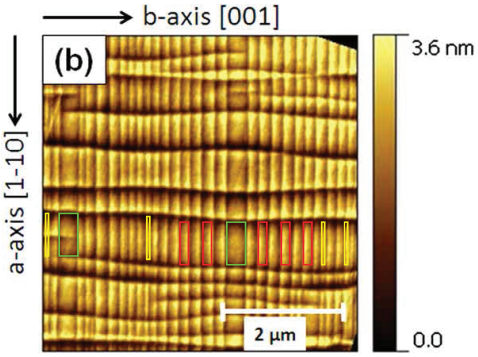

Figure 5.5 *PFM image of $PbTiO_3$ films grown on $DyScO_3$ by Nesterov et al.[14]. Only a select few domain sizes (only considering c-domains here) can be found with an error of about 10 nm. The yellow, red and green rectangles signal some of the 75 nm, 150nm and 300 nm wide domains, respectively.*

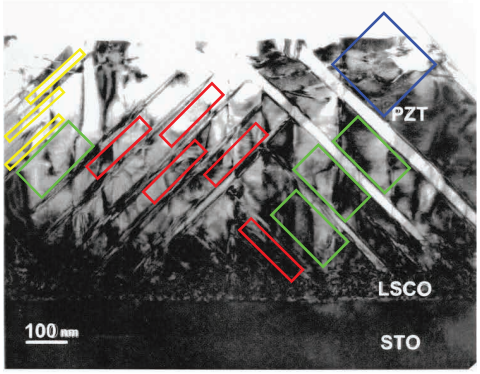

Figure 5.6 *Cross-sectional TEM image of $PbZr_{0.2}Ti_{0.8}O_3$ thin films grown on $SrTiO_3$ by Ganpule et al.[17]. Only a select few domain sizes (only considering c-domains here) can be found with an error of about 5 nm. The yellow, red, green and blue rectangles highlight the 22 nm wide, 44 nm wide, 88 nm wide and 172 nm wide domains, respectively. The domain sizes are defined as the width of the rectangles.*

5.5 Conclusion

To summarize, we have noted that local variations in the domain widths of ferroelastic domains in epitaxial thin films are not statistically spread around the expected equilibrium value (determined by Roytburd's law), nor they are typically related to the presence of random defects. Instead, the observed domain sizes on a given sample are often related by a 2^n factor. We have shown that this can be explained by the kinetics of domain formation: new domains can form upon

cooling (heating) by gradually halving (doubling) the domain periodicity. Thus, deviations from thermodynamic equilibrium allow the observation of frozen domains with discretized widths. This improved knowledge into the mechanism of ferroelastic domain formation can have profound impact in the design of domains and domain wall functionality.

5.6 Note on in-plane domain switching

PFM is able to apply an effective in-plane electric field by scanning the PFM tip over the surface, which is able to give in-plane switching of the domains, as fully explained in Ref.[22]. The in-plane switching in that reference depends on the sign of the DC voltage and the slow-scanning direction of the PFM tip which gives the effective in-plane electric field. The same in-plane switching experiments have been performed on the a/b domains in **Figure 5.7** on the $BaTiO_3$ reported in the paper. It can be seen that it has been possible to switch the direction of the domains and domain walls by the application of the in-plane electric field, since the 2x2 µm area on which the in-plane electric field was applied has all domains along the same direction while that was previously not the case. However, it has not been possible to get a clear relationship between the direction of the in-plane electric field and the subsequent direction of the domain walls after the application of different in-plane electric fields. The only consistent observation is that it is rather easy to rotate the domains towards the most common domain orientation, even when an AC field is applied rather than a DC field. These observations show that the a/b domains can switch direction with just a small driving force, which makes it easier for the material to repair an unfavorable domain orientation after the domains have already been formed.

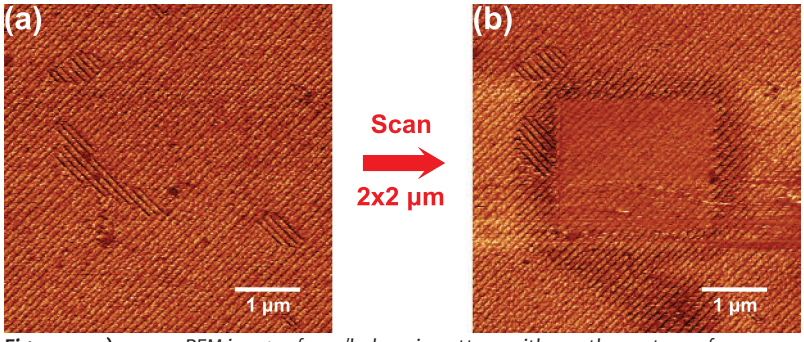

Figure 5.7 a) *5x5 µm PFM image of an a/b domain pattern with mostly one type of domain wall direction, but with a few domains oriented in the perpendicular direction (a superdomain area).* ***b)*** *Same 5x5 µm PFM image after measuring a 2x2 µm in the center (the square that can be seen) with a 2 V DC voltage.*

5.7 References

[1] E. K. H. Salje. *"Ferroelastic Materials."* Annual Review of Materials Research **42,** 265–283 (2012)

[2] A. L. Roitburd. *"Equilibrium structure of epitaxial layers."* Physica Status Solidi (a) **37,** 329–339 (1976)

[3] W. Pompe, X. Gong, Z. Suo and J. S. Speck. *"Elastic energy release due to domain formation in the strained epitaxy of ferroelectric and ferroelastic films."* Journal of Applied Physics **74,** 6012 (1993)

[4] N. A. Pertsev and A. G. Zembilgotov. *"Energetics and geometry of 90 domain structures in epitaxial ferroelectric and ferroelastic films."* Journal of Applied Physics **78,** 6170 (1995)

[5] G. Catalan, J. Seidel, R. Ramesh and J. Scott. *"Domain wall nanoelectronics."* Reviews of Modern Physics **84,** 119–156 (2012)

[6] I. A. Luk'yanchuk, A. Schilling, J. M. Gregg, G. Catalan and J. F. Scott. *"Origin of ferroelastic domains in free-standing single-crystal ferroelectric films."* Physical Review B **79,** 144111 (2009)

[7] J. Fousek, A. K. Tagantsev and L. E. Cross. *"Domains in Ferroic Crystals and Thin Films."* Springer Science + Business Media, Inc. (2011)

[8] G. Catalan, J. F. Scott, A. Schilling and J. M. Gregg. *"Wall thickness dependence of the scaling law for ferroic stripe domains."* Journal of Physics: Condensed Matter **19,** 22201 (2007)

[9] G. Catalan, I. Lukyanchuk, A. Schilling, J. M. Gregg and J. F. Scott. *"Effect of wall thickness on the ferroelastic domain size of $BaTiO_3$."* Journal of Materials Science **44,** 5307–5311 (2009)

[10] A. Schilling, T. B. B. Adams, R. M. Bowman, J. M. Gregg, G. Catalan and J. F. Scott. *"Scaling of domain periodicity with thickness measured in $BaTiO_3$ single crystal lamellae and comparison with other ferroics."* Physical Review B **74,** 24115 (2006)

[11] A. Schilling, R. M. Bowman, G. Catalan, J. F. Scott and J. M. Gregg. *"Morphological control of polar orientation in single-crystal ferroelectric nanowires."* Nano Letters **7,** 3787–3791 (2007)

[12] M. Mtebwa, L. Feigl, P. Yudin, L. J. Mcgilly, K. Shapovalov, A. K. Tagantsev and N. Setter. *"Room temperature concurrent formation of ultra-dense arrays of ferroelectric domain walls."* Applied Physics Letters **107,** 142903 (2015)

[13] G. Catalan, H. Béa, S. Fusil, M. Bibes, P. Paruch, A. Barthélémy and J. F. Scott. *"Fractal dimension and size scaling of domains in thin films of multiferroic $BiFeO_3$."* Physical Review Letters **100,** 27602 (2008)

[14] O. Nesterov, S. Matzen, C. Magen, A. H. G. Vlooswijk, G. Catalan and B. Noheda. *"Thickness scaling of ferroelastic domains in $PbTiO_3$ films on $DyScO_3$."* Applied Physics Letters **103,** 142901 (2013)

[15] D. D. Fong, G. B. Stephenson, S. K. Streiffer, J. A. Eastman, O. Auciello, P. H. Fuoss and C. Thompson. *"Ferroelectricity in ultrathin perovskite films."* Science **304,** 1650–1653 (2004)

[16] G. Catalan, A. Lubk, A. H. G. Vlooswijk, E. Snoeck, C. Magen, A. Janssens, G. Rispens, G. Rijnders, D. H. A. Blank and B. Noheda. *"Flexoelectric rotation of polarization in ferroelectric thin films."* Nature materials **10,** 963–967 (2011)

[17] C. S. Ganpule, V. Nagarajan, H. Li, A. S. Ogale, D. E. Steinhauer, S. Aggarwal, E. Williams, R. Ramesh and P. De Wolf. *"Role of 90° domains in lead zirconate titanate thin films."* Applied Physics Letters **77,** 292 (2000)

[18] S. Y. Hu, Y. L. Li and L. Q. Chen. *"Effect of interfacial dislocations on ferroelectric phase stability and domain morphology in a thin film - a phase-field model."* Journal of Applied Physics **94,** 2542 (2003)

[19] L. J. McGilly, T. L. Burnett, A. Schilling, M. G. Cain and J. M. Gregg. *"Domain annihilation due to temperature and thickness gradients in single-crystal $BaTiO_3$."* Physical Review B **85,** 54113 (2012)

[20] A. S. Everhardt, S. Matzen, N. Domingo, G. Catalan and B. Noheda. *"Ferroelectric Domain Structures in Low-Strain $BaTiO_3$."* Advanced Electronic Materials **2,** 1500214 (2015)

[21] This halving of periodicity ignores the width of the b-domains themselfes, so deviations from this domain periodicity halving are expected when the distance between the b-domains becomes comparable to the b-domain width itself.

[22] S. Matzen, O. Nesterov, G. Rispens, J. A. Heuver, M. Biegalski, H. M. Christen and B. Noheda. *"Super switching and control of in-plane ferroelectric nanodomains in strained thin films."* Nature communications **5,** 4415 (2014)

[23] R. Uecker, B. Velickov, D. Klimm, R. Bertram, M. Bernhagen, M. Rabe, M. Albrecht, R. Fornari and D. G. Schlom. *"Properties of rare-earth scandate single crystals (Re=Nd–Dy)."* Journal of Crystal Growth **310,** 2649–2658 (2008)